

Amplification and squeezing of quantum noise with a tunable Josephson metamaterial

M. A. Castellanos-Beltran,^{1,*} K. D. Irwin,² G. C. Hilton,² L. R. Vale,² and K. W. Lehnert¹

¹*JILA, National Institute of Standards and Technology and the University of Colorado, and Department of Physics, University of Colorado, Boulder, Colorado 80309*

²*National Institute of Standards and Technology, Boulder, Colorado 80305*

(Dated: October 22, 2018)

arXiv:0806.0659v1 [cond-mat.mes-hall] 4 Jun 2008

It has recently become possible to encode the quantum state of superconducting qubits and the position of nanomechanical oscillators into the states of microwave fields^{1,2}. However, to make an ideal measurement of the state of a qubit, or to detect the position of a mechanical oscillator with quantum-limited sensitivity requires an amplifier that adds no noise. If an amplifier adds less than half a quantum of noise, it can also squeeze the quantum noise of the electromagnetic vacuum. Highly squeezed states of the vacuum serve as an important quantum information resource. They can be used to generate entanglement or to realize back-action-evading measurements of position^{3,4}. Here we introduce a general purpose parametric device, which operates in a frequency band between 4 and 8 GHz. It is a subquantum-limited microwave amplifier, it amplifies quantum noise above the added noise of commercial amplifiers, and it squeezes quantum fluctuations by 10 dB.

With the emergence of quantum information processing with electrical circuits, there is a renewed interest in Josephson parametric devices^{5,6,7,8,9}. Previous work with Josephson parametric amplifiers demonstrated that they can operate with subquantum-limited added noise and modestly squeeze vacuum noise^{10,11,12,13,14}. Earlier realizations of Josephson parametric amplifiers (JPAs) were only capable of amplifying signals in a narrow frequency range, were not operated with large enough gain to make the noise of the following, conventional amplifier negligible or were too lossy to be subquantum limited⁵. For related reasons, the degree of squeezing of the vacuum noise was never larger than 3 dB. We create a new type of parametric amplifier in which we embed a tunable, low-loss, and nonlinear metamaterial in a microwave cavity. The tunability of the metamaterial allows us to adjust the amplified band between 4 and 8 GHz, and the cavity isolates the gain medium from low-frequency noise, providing the stability required to achieve high gains and large squeezing.

A single mode of a microwave field with angular frequency ω can be decomposed in two orthogonal components, referred to as quadratures

$$\hat{V}(t) \propto \hat{X}_1 \cos \omega t + \hat{X}_2 \sin \omega t$$

where \hat{X}_1 and \hat{X}_2 are conjugate quantum variables obeying the commutation relation $[\hat{X}_1, \hat{X}_2] = i/2$. The proportionality constant depends on the details of the mode^{15,16,17}. As a consequence of the commutation relation, the uncertainties in \hat{X}_1 and \hat{X}_2 are subject

to the Heisenberg constraint $\Delta X_1 \Delta X_2 \geq 1/4$, where ΔX_j^2 is the variance of the quadrature amplitude \hat{X}_j . A mode is “squeezed” if for one of the quadratures $\Delta X_j < 1/2$ (ref. 17). An amplifier that transforms both input quadratures by multiplying them by a gain \sqrt{G} must add at least half a quantum of noise for the output signal to obey the commutation relation¹⁸; if it adds exactly half a quantum of noise, it is quantum limited. On the other hand, an amplifier which transforms the input signal by multiplying one quadrature by \sqrt{G} and multiplying the other quadrature by $1/\sqrt{G}$ would have an output that satisfies the commutation relation automatically. It need not add any noise to the amplified output mode and, in that sense, can be subquantum limited^{18,19}. A degenerate parametric amplifier transforms the input signal in this way, amplifying one quadrature while deamplifying the other¹⁹.

Our realization of the parametric amplifier consists of a metamaterial embedded in a half-wavelength microwave cavity. The metamaterial is a superconducting niobium coplanar waveguide in which the center conductor is a series array of 480 Josephson junctions. Each junction has been split into two junctions in parallel, forming a SQUID and making the phase velocity of the metamaterial tunable with magnetic flux enclosed by the SQUID loop²⁰ (Fig. 1a). In addition to being flux-tunable, the phase velocity depends on the intensity of the fields propagating in this nonlinear metamaterial¹⁴. (The tunability and nonlinearity of this metamaterial were studied in a preliminary device, fabricated from aluminum, which was too lossy to be subquantum limited or to create highly squeezed states⁵.) We define the cavity by interrupting the center conductor with two capacitors. One capacitor is larger than the other, creating a strongly coupled port and a weakly coupled port.

We operate the parametric amplifier by injecting an intense pump tone into the weakly coupled port at a frequency close to the cavity’s half-wave resonance. Through the intensity-dependant phase velocity, the pump causes the cavity’s resonance frequency to vary at twice the pump’s frequency providing parametric gain. A signal incident on the strongly coupled port is reflected and will be amplified if it is in phase with the pump but deamplified if it is 90 degrees out of phase with the pump. Signals exiting port 2 are further amplified by a chain of commercial amplifiers. We resolve the components of the amplified signal that are in phase I and 90 degrees out of phase Q by mixing the signal with a phase reference called the local oscillator (LO). Because the LO is derived from the same generator that produces the pump, I and Q are simply related to the quadrature components \hat{X}_1 and \hat{X}_2 of the

microwave field exiting port 2. They are related by $I = A(\hat{X}_1 \cos \theta - \hat{X}_2 \sin \theta + \xi_I(t))$ and $Q = A(\hat{X}_1 \sin \theta + \hat{X}_2 \cos \theta + \xi_Q(t))$, where A is the total gain of the commercial amplifiers and mixer, θ is the phase between the pump and the LO, and ξ_I and ξ_Q are random variables. Both random variables have a power spectral density N_A , where N_A is the noise number¹⁸ of the commercial amplifier chain expressed as noise added at the input of the HEMT (see Methods).

Before operating the device as a parametric amplifier, we first characterize its linear behaviour. In Fig. 2a, we measure the cavity's response both by measuring the reflectance of a signal on port 2 and the transmittance from port 1 to port 2 as functions of frequency. The powers used are low enough so that the cavity's response is still linear. From this measurement we can extract the cavity's resonance frequency f_{res} , the rates γ_{c1} and γ_{c2} at which the cavity loses power through both ports as well as through internal loss processes γ_i (Fig. 2a). When operating as a parametric amplifier, the center of the amplified band will be close to f_{res} , and the unity gain signal bandwidth will be approximately $\gamma_{c1} + \gamma_{c2} + \gamma_i$ ^{5,6}. By applying magnetic flux we can move the center of the amplified band over a large range of frequencies (Fig. 2b).

After characterizing the linear response of the device, we operated it as an amplifier. In previous work, we studied the dependence of the parametric gain on the pump power and pump frequency in our first realization of this metamaterial⁵, finding good agreement with the theory in ref. 6. Here we study the JPA's added noise as a function of the cavity's resonance frequency and the total noise of the amplifier chain as a function of the JPA gain. By switching between two calibrated noise sources (Fig. 1a), we can change the incident noise on the JPA. The change in noise power at the output of the mixer allows us to measure the noise N_{JPA} added by the JPA, the JPA gain \sqrt{G} , the total added noise of both the JPA and the commercial amplifier chain N_{tot} (i.e., the total noise referred to the input of the JPA), and the total gain $\sqrt{G}A$. The calibrated noise sources are derived from two resistors held at different temperatures. The resistances are matched to the wave impedance of the cables that carry signals to the JPA input. The noise emitted by both resistors is attenuated by a 10 dB attenuator held at a temperature $T_A = 15$ mK and then passed to the JPA through a microwave circulator which separates the incident and reflected signals from the JPA. The power spectral density in units of noise quanta incident on the

JPA through the circulator is

$$N(T_R) = \frac{1}{2} + \left(\frac{9}{10}\right) \frac{1}{e^{\frac{\hbar\omega}{k_B T_A}} - 1} + \left(\frac{1}{10}\right) \frac{1}{e^{\frac{\hbar\omega}{k_B T_R}} - 1}, \quad (1)$$

where $T_R = T_c = 15$ mK or $T_R = T_h = 4.1$ K depending on the position of the switch shown in Fig. 1a. The first term in equation (1) is the quantum noise while the second and third terms are the thermal noise which is small compared to the quantum noise at $T_R = T_c$. Most of the noise incident on the JPA is $N(T_R)$, but a small amount comes from the coupled port of the directional coupler (see Methods). By selecting $\theta = 0$, the amplified quadrature appears at the I port of the mixer (Fig. 3a). We measure the ratio Y of the noise power at the output I with the hot load incident on the JPA divided by the noise power with the cold load incident on the JPA. This measurement, known as a Y -factor measurement, allows us to extract $N_{\text{tot}} = (N(T_h) - YN(T_c))/(Y - 1)$ and the total gain $A\sqrt{G}$. We then adjust the cavity's resonance frequency about 10 linewidths away from the LO frequency and turn off the pump. Because the JPA now acts as a passive mirror, we can perform a Y -factor measurement on our commercial amplifier chain, finding N_A and A . From both measurements, we extract the JPA gain \sqrt{G} and N_{JPA} (Fig. 3). As observed in Fig. 3b, our JPA adds less than 1/2 a quantum of noise over the 4 – 8 GHz band where it operates. In addition, it can be operated at large enough gain to amplify the quantum noise above the commercial amplifier's noise (Fig. 3c)!

In order to show that the JPA can squeeze quantum noise, we examine the squeezed quadrature X_2 when the incident noise is mostly quantum noise ($T_R = T_c$). When $\theta = 0$, X_2 appears at the Q port. The noise at the Q port referred to the input of the HEMT is composed of the added noise of the commercial amplifiers ($N_A \approx 26$) and noise coming from port 2, $2\Delta X_Q^2$, where $\Delta X_Q^2 = \Delta X_1^2 \sin^2 \theta + \Delta X_2^2 \cos^2 \theta$. When $\theta = 0$, we observe a reduction in ΔX_Q when the pump is turned on, demonstrating that the JPA has squeezed quantum noise (Fig. 4a). As we increase the JPA gain, we observe an increase in the noise squeezing up to $G = 16$ dB (Fig. 4b). For $G < 16$ dB the squeezing we observe is consistent with the expected behaviour from a model of parametric amplification that includes loss in the JPA but no other imperfections⁶. However, for $G > 16$ dB we observe less than the predicted squeezing probably due to the instability in the phase acquired by the pump as it passes through the cryostat in the several minutes required to complete one measurement. Finally, to illustrate the JPA's unequal effect on the noise of the two quadratures, we define

a quantity $\eta(\theta) = (\Delta X_Q^2)_{\text{pump on}} / (\Delta X_Q^2)_{\text{pump off}}$. In Fig. 4c, we plot $\eta(\theta)$ demonstrating that the fluctuations at the output of the JPA are indeed squeezed along the axis defined by the pump (Fig. 3a).

The measurement of the squeezed state would have proceeded much more rapidly if we had used a subquantum limited amplifier, such as a second JPA, instead of a HEMT amplifier. For most measurements, the low added noise of the JPA is helpful, but for some measurements it is crucial. For example, to fully characterize the quantum state of non-Gaussian states, such as the Fock states generated by superconducting qubits², a subquantum limited amplifier is a necessity²¹. In addition to characterizing non-Gaussian states of microwave fields, the JPA is also well suited to amplifying the signal generated by a nanomechanical beam moving in a microwave cavity¹, enabling a quantum-limited measurement of position. The tunability of the amplifier demonstrated here also makes it well suited to use with the increasingly popular frequency-division-multiplexed microwave circuits^{1,22,23} when simultaneous measurement of all frequency channels is not required.

Methods

Devices are fabricated at NIST Boulder using a standard Nb/AlOx/Nb trilayer process²⁴, modified by eliminating the shunt resistor layer and minimizing deposited oxides²³. The device studied here was coprocessed with 10 other devices used for dc characterization. These dc-measurements indicate an average critical current I_c per SQUID in the JPA of 31 μA , which was close to the designed value of 30 μA . The transmission lines from which the half-wavelength cavities were built were designed to have a capacitance per unit length of $C_l = 0.15$ nF/m and a geometrical inductance per unit length of $L_l = 0.49$ $\mu\text{H}/\text{m}$. For $I_c = 31$ μA , the Josephson inductance per SQUID is $L_J = 10.6$ pH. These values predicts a half-wave resonance frequency of 8.23 GHz, when no flux is applied, which is within 3% of the observed value. Measurements were performed in a magnetically shielded dilution refrigerator. To avoid unknown loss and noise in the cables carrying the calibrate noise signals, superconducting Niobium coaxial cables were used to carry these signals between the 15 mK region of the refrigerator and 4 K region. A calibrated ruthenium oxide thermometer measured the refrigerators base temperature and the temperature of the helium bath, to which the 4 K resistor and microwave switch were thermally anchored. A calibration tone,

(Fig. 1a) is used: to verify the gain inferred from the Y -factor measurements, to ensure that the noise reduction arises from genuine squeezing and not saturation of the amplifiers, and to measure S_{22} in the network analysis. The complete expression for the noise incident on the JPA includes contributions from the thermal noise introduced with the calibration tone and the insertion loss of the directional coupler and the switch. The unknown insertion loss at cryogenic temperatures of the directional coupler and of the microwave switch are the dominant uncertainties in the added noise and squeezing measurements. The extreme values represented by the error bars are derived by assuming: first, that there is no insertion loss, and then, that the insertion loss has not changed between room temperature and the operating temperature. Noise at the I or the Q ports is expressed as the double-side-band power-spectral-density referred to the input of the relevant amplifier. Dividing the spectral density by hf_{LO} , yields the noise in dimensionless units of noise quanta, where LO is the local oscillator frequency; e.g. the thermal noise of a resistor at temperature $T \gg hf_{\text{LO}}/k_B$ measured at the I -port would have a noise $N_T = k_B T / hf_{\text{LO}}$.

Acknowledgements

The authors acknowledge funding from the National Institute of Standards and Technology (NIST), from the National Science Foundation, and from a NIST-University of Colorado seed grant. We thank S. M. Girvin, J. D. Teufel, C. A. Regal, N. E. Flowers-Jacobs, J. K. Thompson and M. Holland for valuable conversations and technical assistance. K. W. Lehnert is a member of NIST's Quantum Physics Division.

Competing financial interests

The authors declare that they have no competing financial interests.

* Electronic mail: castellm@colorado.edu

¹ Regal, C. A., Teufel, J. D. & Lehnert, K. W. Measuring nanomechanical motion with a microwave cavity interferometer (2008). ArXiv:0801.1827v2 [quant-ph].

- ² Houck, A. A. *et al.* Generating single microwave photons in a circuit. *Nature(London)* **449**, 328–331 (2007).
- ³ Braunstein, S. L. & van Loock, P. Quantum information with continuous variables. *Rev. Mod. Phys.* **77**, 513–577 (2005).
- ⁴ Caves, C. M., Thorne, K. S., Drever, R. W. P., Sandberg, V. D. & Zimmermann, M. On the measurement of a weak classical force coupled to a quantum-mechanical oscillator. I. Issues of principle. *Rev. Mod. Phys.* **52**, 341–392 (1980).
- ⁵ Castellanos-Beltran, M. A. & Lehnert, K. W. Widely tunable parametric amplifier based on a superconducting quantum interference device array resonator. *Appl. Phys. Lett.* **91**, 083509 (2007).
- ⁶ Yurke, B. & Buks, E. Performance of cavity-parametric amplifiers, employing kerr nonlinearities, in the presence of two-photon loss. *J. Lightw. Technol.* **24**, 5054–5066 (2006).
- ⁷ Tholén, E. A. *et al.* Nonlinearities and parametric amplification in superconducting coplanar waveguide resonators. *Appl. Phys. Lett.* **90**, 253509 (2007).
- ⁸ Siddiqi, I. *et al.* Rf-driven Josephson bifurcation amplifier for quantum measurement. *Phys. Rev. Lett.* **93**, 207002 (2004).
- ⁹ Zagoskin, A., Il'ichev, E., McCutcheon, M. W., Young, J. & Nori, F. Generation of squeezed states of microwave radiation in a superconducting resonant circuit (2008). ArXiv:0804.4186v1 [cond-mat.supr-con].
- ¹⁰ Yurke, B. Squeezed-state generation using a Josephson parametric amplifier. *J. Opt. Soc. Am. B* **4**, 1551–1557 (1987).
- ¹¹ Yurke, B. *et al.* Observation of 4.2-k equilibrium-noise squeezing via a Josephson-parametric amplifier. *Phys. Rev. Lett.* **60**, 764–767 (1988).
- ¹² Yurke, B. *et al.* Observation of parametric amplification and deamplification in a Josephson parametric amplifier. *Phys. Rev. A* **39**, 2519–2533 (1989).
- ¹³ Movshovich, R. *et al.* Observation of zero-point noise squeezing via a Josephson-parametric amplifier. *Phys. Rev. Lett.* **65**, 1419–1422 (1990).
- ¹⁴ Yurke, B., Roukes, M. L., Movshovich, R. & Pargellis, A. N. A low-noise series-array Josephson junction parametric amplifier. *Appl. Phys. Lett.* **69**, 3078–3080 (1996).
- ¹⁵ Yurke, B. & Denker, J. S. Quantum network theory. *Phys. Rev. A* **29**, 1419–1437 (1984).
- ¹⁶ Louisell, W. H. *Radiation and Noise in Quantum Electronics*, chap. 4, 137–174 (McGraw-Hill

- Book Company, New York, 1964).
- ¹⁷ Gerry, C. C. & Knight, P. L. *Introductory Quantum Optics* (Cambridge University Press, Cambridge, UK, 2006).
 - ¹⁸ Caves, C. M. Quantum limits on noise in linear amplifiers. *Phys. Rev. D* **26**, 1817–1839 (1982).
 - ¹⁹ Takahasi, H. *Advances in Communication Systems*, edited by Balakrishnan, A. V., chap. 6, 227–310 (Academic Press, New York, 1965).
 - ²⁰ Haviland, D. B. & Delsing, P. Cooper-pair charge solitons: The electrodynamics of localized charge in a superconductor. *Phys. Rev. B* **54**, R6857–R6860 (1996).
 - ²¹ Yurke, B. & Stoler, D. Generating quantum mechanical superpositions of macroscopically distinguishable states via amplitude dispersion. *Phys. Rev. Lett.* **57**, 13–16 (1986).
 - ²² Day, P. K., LeDuc, H. G., Mazin, B. A., Vayonakis, A. & Zmuidzinas, J. A broadband superconducting detector suitable for use in large arrays. *Nature (London)* **425**, 817–821 (2003).
 - ²³ Mates, J. A. B., Hilton, G. C., Irwin, K. D., Vale, L. R. & Lehnert, K. W. Demonstration of a multiplexer of dissipationless superconducting quantum interference devices. *Appl. Phys. Lett.* **92**, 023514 (2008).
 - ²⁴ Sauvageau, J. *et al.* Superconducting integrated circuit fabrication with low temperature ECR-based PECVD SiO₂ dielectric films. *IEEE Trans. Appl. Supercond.* **5**, 2303 – 2309 (1995).

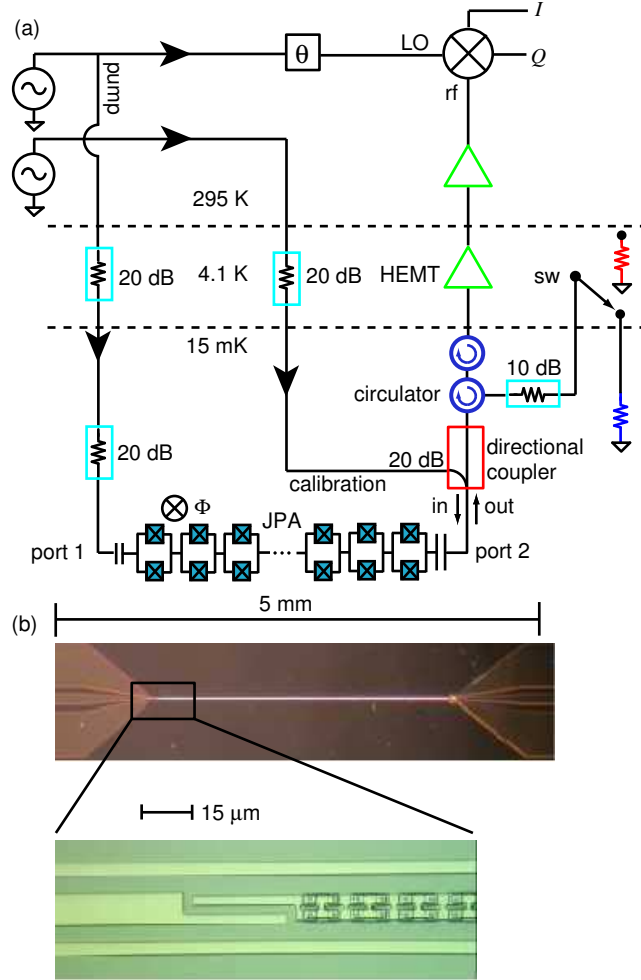


FIG. 1: **Measurement schematic and device images.** **a**, The JPA is measured in a cryostat held at 15 mK. Two microwave generators are used to study the JPA. One generator creates the pump and LO tones, while the second creates a calibration tone. The pump tone is injected through port 1 of the JPA, while the calibration tone is incident on port 2 of the JPA through a 20 dB direction coupler. Signals emerging from port 2 pass through a circulator and are then amplified by a cryogenic high-electron-mobility transistor amplifier (HEMT) and a room temperature amplifier before entering the radio-frequency (rf) port of a mixer. The noise incident on port 2 of the JPA which comes primarily from the isolated port of the circulator can be switched (sw) to come from two different resistors held at different temperatures. **b**, The images are a picture of the full device (upper) and a magnified image of the weakly coupled port and a few SQUIDS (lower).

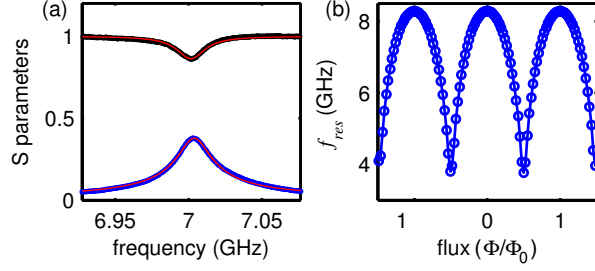


FIG. 2: **Linear response of the JPA.** **a**, We plot the fraction of microwave amplitude transmitted from port 1 to port 2 $|S_{21}|$ (blue) and the fraction reflected from port 2 $|S_{22}|$ (black) as functions of frequency at a particular value of applied magnetic flux. By fitting this data to a model of a two port cavity (red lines), we extract $f_{res} = 7.0038$ GHz, $\gamma_{c1} = 2\pi \times 437$ kHz, $\gamma_{c2} = 2\pi \times 10.55$ MHz, and $\gamma_i = 2\pi \times 341$ kHz. **b**, We plot the measured value of f_{res} as a function of applied magnetic flux Φ in units of the magnetic flux quantum Φ_0 . We use the obvious periodicity in this data to infer the magnetic flux enclosed by the SQUIDs.

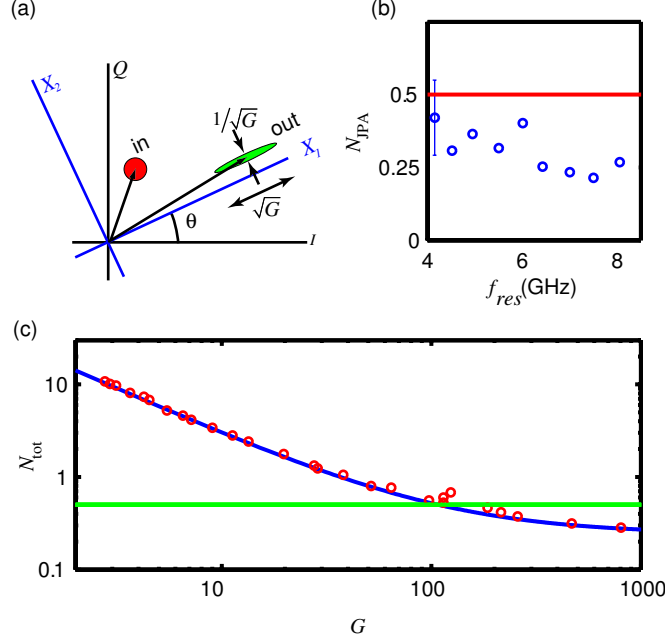


FIG. 3: **Added noise of the JPA and of the full measurement chain.** **a**, This diagram represents the operation of an ideal degenerate parametric amplifier which transforms an input state (red circle) into an output state (green ellipse) by amplifying the X_1 component by \sqrt{G} and squeezing the X_2 component by $1/\sqrt{G}$. The mixer projects the output state into axes rotated by θ . **b**, We measure N_{JPA} at nine different values of f_{res} between 4 and 8 GHz and observe that the added noise is less than half a quantum (red line). The error bar applies to all points; it represents the systematic uncertainty introduced primarily by the unknown loss of the directional coupler and switch when operated cryogenically. **c**, We plot N_{tot} when $f_{\text{res}} = 7.00$ GHz versus G (points). At this frequency $N_A = 26$ and is dominated by the HEMT. With increasing G , this noise becomes negligible compared to $N_{\text{JPA}} = 0.23$, where we expect $N_{\text{tot}} = N_{\text{JPA}} + N_A/G$ (blue line). At the largest gains $N_{\text{tot}} < 0.5$ (green line) and $N_A/G = 0.04$.

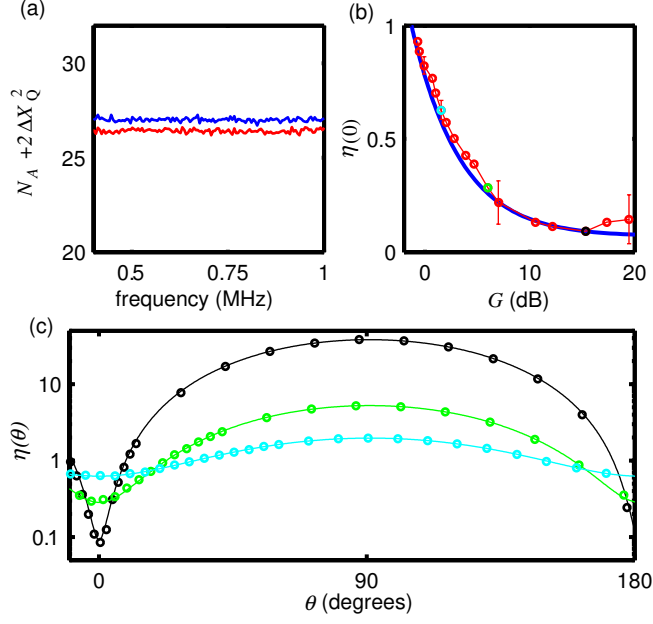


FIG. 4: **Demonstration of squeezing.** **a**, Power spectral density versus frequency at the Q output of the mixer referred to the input of the commercial amplifier chain in units of quanta, measured with the pump on (red) and the pump off (blue) for $\theta = 0$, $f_{res} = 7$ GHz and $G = 15.3$ dB. **b**, The squeezing $\eta(0)$ as a function of G (points) and the predicted squeezing from reference 6 (line). The error bars represent the same systematic error as in Fig. 3b. This uncertainty varies smoothly between the error bars shown in selected data points. **c**, $\eta(\theta)$ as a function of θ for three different gains (points) for $G = 34$ (black), $G = 4$ (green), $G = 1.4$ (cyan) and the expected θ dependance (lines)^{6,12}.